Evolution and genetic architecture of disassortative mating at a locus under heterozygote advantage

Ludovic Maisonneuve[1,*], Mathieu Joron[2], Mathieu Chouteau[3] and Violaine Llaurens[1]

1. Institut de Systematique, Evolution, Biodiversité (ISYEB), Museum National d'Histoire Naturelle, CNRS, Sorbonne-Université, EPHE, Université des Antilles, 45 rue Buffon, 75005 Paris, France;

2. Centre d'Ecologie Fonctionnelle et Evolutive, UMR 5175 CNRS-Université de Montpellier, École Pratique des Hautes Études, Université Paul Valéry, 34293 Montpellier 5, France;

3. Laboratoire Ecologie, Evolution, Interactions Des Systèmes Amazoniens (LEEISA), USR 3456, Université De Guyane, IFREMER, CNRS Guyane, 275 route de Montabo, 97334 Cayenne, French Guiana;

∗ Corresponding author: Ludovic Maisonneuve; e-mail: ludovic.maisonneuve@mnhn.fr.

Manuscript elements: Table 1, figure 1, figure 2, figure 3, figure 4, figure 5, figure S1, figure S2, figure S3, figure S4,figure S5 , figure S6, figure S7, figure S8.

Keywords: Heterogamy, Supergene, Frequency dependent selection, genetic load, mate preference, *Heliconius numata*.

Manuscript type: Article.

Abstract

The evolution of mate preferences may depend on natural selection acting on the mating cues and on the underlying genetic architecture. While the evolution of assortative mating acting on locally adapted traits has been well-characterized, the evolution of disassortative mating is poorly characterized. Here we aim at understanding the evolution of disassortative mating for traits under strong local selection, by focusing on polymorphic mimicry as an illustrative example. Positive frequency-dependent selection exerted by predators indeed generates positive selection on mimetic colour patterns. In this well-characterized adaptive landscape, polymorphic mimicry is rare but had been reported in a butterfly species where chromosomal inversions control mimetic colour pattern variations. Because inversions are often associated with recessive deleterious mutations, we hypothesize they may induce a heterozygote advantage at the colour pattern locus, putatively favoring the evolution of disassortative mating. To explore the conditions underlying the emergence of disassortative mating, we modeled both a color pattern locus and a mate preference locus. We confirm that a heterozygote advantage favors the evolution of disassortative mating and show that disassortative mating is more likely to emerge if at least one adaptive allele is free from any genetic load. Comparisons of hypothetical genetic architectures underlying mate choice behaviors show that rejection alleles linked to the colour pattern locus can be under positive selection and enable the emergence of disassortative mating behaviour. Our results therefore provide relevant predictions on both the selection regimes and the genetic architecture favouring the emergence of disassortative mating, which could be compared to empirical data that are starting to emerge on mate preferences in wild populations.

Introduction

Mate preferences often play an important role in shaping traits diversity in natural populations, but the mechanisms responsible for their emergence often remain to be characterized. While the evolution of assortative mating on locally adapted trait is relatively well understood (Otto et al., 2008; de Cara et al., 2008; Thibert-Plante and Gavrilets, 2013), the selective forces involved in the evolution of disassortative mating are still largely unknown. Disassortative mating, *i.e.* preferential crosses between individuals displaying a different phenotype, is a rare form of mate preference (Jiang et al., 2013) and is expected to have a large effect on polymorphism in traits targeted by sexual selection. In populations where individuals tend to mate with partners with a phenotype different from their own, individuals with a rare phenotype have a larger number of available mates, resulting in higher reproductive success. By generating a negative frequency-dependent selection on mating cues, disassortative mating is thus often pointed out to generate and/or maintain polymorphism within populations of various species. Obligate disassortative mating for sexes or mating types leads to the persistence of intermediate frequencies of sexes or mating types (Wright, 1939), and promotes polymorphism, with in some extreme cases, thousands of mating types being maintained, as in some Basidiomycete fungi for instance (Casselton, 2002). A few examples of disassortative mating are also based on other traits such as body chirality in Amphridromus inversus snails, where a greater fecundity is reported in inter-chiral mating events, therefore promoting polymorphism within population (Schilthuizen et al., 2007). Disassortative mating is frequently reported in traits where polymorphism is maintained because of natural selection: in the scale eating predator fish Perissodus microlepis, a dimorphism on the mouth-opening direction ('lefty' versus 'righty') is maintained within populations by negative frequency-dependent selection (Takahashi and Hori, 2008), due to prey behavior monitoring the most attacked side. A disassortative mating behavior based of the mouth-opening direction is also observed in this species (Hori, 1993). Disassortative mating based on odors is also reported in mice (Penn and Potts, 1999) and humans (Wedekind et al., 1995): odor profiles are indeed

tightly linked to genotypes at the MHC loci controlling for variations in the immune response, known to be under strong balancing selection (Piertney and Oliver, 2006). The balancing selection in MHC partly stems from heterozygous advantage, whereby heterozygous genotypes might be able to recognize a large range of pathogens. Such heterozygote advantage may thus promotes the evolution of disassortative mating (Tregenza and Wedell, 2000). Extreme examples of heterozygotes advantage are observed for loci for which homozygotes have reduced survival. In the seaweed fly Coelopa frigida the heterozygotes ($\alpha\beta$) at the locus Adh have a better fitness than homozygotes ($\alpha\alpha$ or $\beta\beta$) (Butlin et al., 1984; Mérot et al., 2019) and females prefer males with a different genotype on Adh locus from their own (Day and Butlin, 1987). In the white-throated sparrow *Zonotrichia albicollis*, strong disassortative mating is reported regarding the color of the head stripe and associated with chromosomal dimorphism. This plumage polymorphism is controlled by single locus (Tuttle et al., 2016), where a lack of homokaryotype individuals is observed (Horton et al., 2013).

Nevertheless while the fitness advantage of disassortative mating at loci with overdominance seems straightforward, the genetic basis of disassortative mating preferences remains largely unknown. One exception is the self-incompatibility system in *Brassicaceae* where the S-locus controls for a specific rejection of incompatible pollen (Hiscock and McInnis, 2003). S-haplotypes contains tightly linked co-evolved SCR and SRK alleles, encoding for a protein of the pollen coat and a receptor kinase located in the pistil membrane respectively, preventing fertilization from self-incompatible pollen due to specific receptor-ligand interactions. Self-rejection is also suggested to explain the disassortative mating behavior linked to odor in humans. Body odors are strongly influenced by genotypes at the immune genes HLA and rejection of potential partners is shown to be linked to level of HLA similarity, rather than specific rejection of a given HLA genotype (Wedekind and Füri, 1997). In the white-throated sparrow, disassortative mating stems from specific preferences for color plumage that differ between males and females, whereby tan-striped males are preferred by all females whereas white-striped females are preferred by all males (Houtman and Falls, 1994). Different mechanisms leading to mate preferences and as-

sociated genetic architecture can thus be hypothesized, that could depend (1) or not (2) on the phenotype of the chooser. Based on the categories described by Kopp et al. (2018), we assume either (1) *Self-referencing*, (*i.e.* when individual used its own signal to choose its mate), that could involve either (1a) a single locus affecting both the mating cues and the preferences or (1b) a two locus architecture where one locus controls mating cues and the second one encodes for a mating behavior that depends on the phenotype at the trait locus or (2) preferences for or rejection of a given phenotype (*preference/trait* hypothesis), that could involve two loci, one controlling the mating cue and the other the preference toward the different cues (Kopp et al., 2018). The locus controlling preference could therefore either be the same or different from the locus controlling cue variations, and in the latter case, the level of linkage disequilibrium between the two loci could have a strong impact on the evolution of disassortative mating. The level of recombination between loci controlling mating cues and mating preferences potentially has a strong impact on the evolution of mate behavior, and these two main categories become quite similar when the linkage disequilibrium is high. In models investigating the evolution of assortative mating on locally-adapted traits, theoretical simulations have demonstrated that assortative mating is favored when the preference and the cue locus are linked (Kopp et al., 2018).

Here we explore the evolutionary forces leading to the emergence disassortative mating behaviour. We focus on the specific case of the butterfly species *Heliconius numata*, where high polymorphism in wing pattern is maintained within population (Joron et al., 1999) and strong disassortative mating is documented between wing pattern forms (Chouteau et al., 2017). *H. numata* butterflies are chemically-defended (Arias et al., 2016), and their wing patterns act as warning signals against predators. At a local scale, natural selection leads to the fixation of a single warning signal shared among sympatric defended species (Müllerian mimicry) (Merrill et al., 2015). However, local polymorphism of mimetic colour patterns can still emerge within species in some balancing conditions between migration and local selection for specific mimetic patterns (Joron and Iwasa, 2005). The local polymorphism of several mimetic patterns observed within populations of H. numata (Joron et al., 1999), would then require a high migration rate

compensating for strong local selection. However, disassortative mating based on wing pattern is reported in *H. numata* in which females reject males displaying the same color pattern (Chouteau et al., 2017). Such disassortative maring behaviour could then enhance the local polymorphism in colour pattern within this species. This mating behavior could, in turn, promote migration because immigrant individuals exhibiting a locally rare phenotype would benefit from increased reproductive success. Nevertheless, the evolution of such disassortative mating is unclear, notably because this mate preference should be strongly counter-selected by predators attacking more readily locally rare, non-mimetic warning patterns (Chouteau et al., 2016). By focusing on this well-documented example, we used a theoretical approach to provide general predictions on the evolution of disassortative mating in polymorphic traits, and on expected genetic architecture underlying this behavior.

Variation in wing colour patterns of H. numata is controlled by a single genomic region, called the supergene P (Joron et al. , 2006), which display chromosomal inversions (Joron et al. , 2011). These inversions have recently been shown to be associated with a significant genetic load, resulting in a strong heterozygote advantage (Jay et al, bioRxiv). We thus investigate whether genetic load associated with locally adaptive alleles may favor the evolution of mate preference and promote local polymorphism despite local directional selection. We then explored two putative genetic architectures of mate preferences based on (1) *self referencing* and (2) based on *preference/trait* rule, and tested their respective impact on the evolution of disassortative mating behavior. Under both hypotheses, we assumed that the mating cue and the mating preference are controlled by two distinct loci, and investigate the effect of linkage between loci on the evolution of disassortative mating behavior.

Methods

Based on a previous-developed model of Müllerian mimicry (Joron and Iwasa, 2005) extended to diploid populations (Llaurens et al., 2013), we describe a two-populations model with a locus *P*

controlling mimetic color pattern under local selection and spatial variations in mimetic communities, leading to opposite local selection on color pattern in the two populations. We explicitly model the genetic architecture controlling mate preference toward color pattern by a locus M assuming either (1) a preference based on the phenotype of the choosing individual or (2) a preference for a given color pattern displayed by mating partner, independent from the colour pattern of the choosing individual. We also assume different levels of genetic load associated with the color pattern alleles. Every individual thus have a genotype i described as follows :

$$i = (p_1, p_2, m_1, m_2), \tag{1}$$

where p_1 and p_2 are two alleles at the locus P and m_1 and m_2 two alleles at the locus M.

We track down the evolution of allele frequencies at both the locus P controlling variations in wing color pattern and locus M controlling mate preference. A recombination rate r between these two loci is assumed.

Mimetic color patterns

At locus P, three alleles are assumed to segregate, namely alleles a, b and c, encoding for phenotypes [A], [B] and [C] respectively. We assume strict dominance among the three alleles with a ¿ b ¿ c in agreement with the strict dominance observed among supergene P alleles within natural populations of H. numata (Le Poul et al., 2014). The three color pattern phenotypes are assumed to be perceived as strictly different by both mating partners and predators. The resemblance Res[i][j] between pairs of individuals exhibiting phenotype [i] and [j] respectively is thus set to 1 for identical phenotypes and to 0 for dissimilar one. The resemblance matrix among the three phenotypes is :

$$Res = \begin{pmatrix} 1 & 0 & 0 \\ 0 & 1 & 0 \\ 0 & 0 & 1 \end{pmatrix}$$

Spatial variation in mimetic communities

Local selection promotes convergent evolution of wing color pattern among defended species (i. e. Müllerian mimicry, (Müller, 1879)), forming so-called mimicry rings composed of individuals from different species displaying the same warning signal. At a larger scale, a spatial mosaic of warning patterns can be observed, through an equilibrium between colonization and selection acting locally (Sherratt, 2006).

Here we assume two populations of an unpalatable species involved in Müllerian mimicry with other chemically-defended species. We assume separated sex and obligate sexual reproduction between the two sexes. The environment differs in communities of local species involved in mimicry (*i.e.* mimicry rings). We consider two patches occupied by different mimetic communities: population 1 is located in a patch where the local community (*i.e.* other chemically-defended species, not including *H. numata*) mostly displays phenotype [A], and population 2 in a patch where the mimetic community mostly displays phenotype [B]. This spatial heterogeneity is represented by the parameter $\sigma \in [0, 1]$ simulating the relative proportion of phenotypes [A] and [B] in mimicry rings of patch 1 and 2 respectively, so that the higher is σ, the more the two communities differed, leading to spatial heterogeneity favouring phenotype [A] in patch 1 and phenotype [B] in patch 2. This spatial heterogeneity σ plays a central role on the predation suffered by the different phenotypes in the two patches (see Predation section below). The focal mimetic species is polymorphic for those two phenotypes, corresponding to the locally advantageous phenotypes [A] or [B] (Note that the allele c, and corresponding phenotype [C] is non-mimetic in both patches and is then disadvantaged in both patches).

Positive frequency-dependent predation

Every individual of the focal (polymorphic) species suffer a predation risk modulated by its resemblance to the local mimetic community of butterflies. We assume a symmetrical condition where the mortality coefficient was $d(1 - \sigma)$ for phenotypes matching the local mimicry ring

(*i.e.* diminishing predation exerted on genotypes displaying phenotype [A] in population 1 and genotypes displaying [B] in population 2) and $d(1+\sigma)$ otherwise (*i.e.* increasing predation exerted on genotypes displaying phenotype [B] or [C] in population 1 and on genotypes displaying phenotype [A] or [C] in population 2), where d represents the baseline predation risk and σ the spatial heterogeneity of mimicry communities in patch 1 and 2.

Predation exerted on a given phenotype depends on its match to the local mimicry environment, but also on its own abundance in the patch. Predators learn to associate warning patterns to chemical defense. This learning behavior generates a positive frequency-dependent selection (pFDS) on butterfly wing pattern (Chouteau et al., 2016), because displaying a widely shared color pattern decreases the risk of encountering a naive predator (Sherratt, 2006). Number-dependent predator avoidance in the focal species is assumed to depend on its unpalatability coefficient (λ) and the density of each phenotype, so that protection gained by resemblance among phenotypes is greater for higher values of the unpalatability coefficient λ. This results in the following change in number of each genotype i in population pop due to predation :

$$\Delta P^t_{i,pop} = -\frac{d}{1+\lambda(\sum_j Res_{[i],[j]})N^t_{j,pop}}[(1+\sigma)(1-Res_{[i],[pop]}) + (1-\sigma)Res_{[i],[pop]}]N^t_{i,pop} \quad (2)$$

with $N_{i,pop}$ representing the total number of individuals with genotype i in population pop, $Res_{[i],[pop]}$ representing the resemblance of the phenotype expressed by genotype i to the local mimetic community. The predation rate is indeed lower in individuals displaying the phenotype mimetic to the local community (*i.e.* the phenotype A in population 1 and B in population 2). Individuals displaying phenotype [C] were non-mimetic in both populations, and therefore suffer from high predation risk in both populations. The numerator models the positive number dependent selection, this effect being stronger for higher values of toxicity.

Migration

The change in the number of individuals with genotype i in population pop due to migration between populations pop and pop' is given by:

$$\Delta M^{t}_{i,pop} = mig(N_{i,pop'} - N_{i,pop}) \tag{3}$$

with mig is the migration coefficient $mig \in [0, 1]$).

Mate preferences

The mate preference is considered as strict, implying that choosy individuals never mate with individuals displaying a non-preferred phenotype. Two hypothetical mate preference mechanisms are investigated. Under the *self-referencing* hypothesis (hyp 1), two alleles are assumed at loci M, coding for (i) random mating (r) and (ii) preferential mating behavior (either assortative *sim* or disassortative *dis*) respectively (see fig. S1 for more details). We assume that the preference alleles sim and dis are dominant over the random mating allele r (see fig. S1 for more details). The dominance relationships between the sim and dis alleles are not specified because we investigate independently the evolution of assortative and disassortative mating from a population ancestrally mating at random. Note that under hyp. 1, mating behavior is based on a self-referencing, and thus crucially depends on the color pattern of the individual expressing the preference.

An alternative model of mechanisms of mate preference is investigated, assuming a specific recognition of color patterns, acting as mating cue (*preference/trait*, hyp.2). Under hyp.2, four alleles segregate at locus M: allele M_r, coding for an absence of color pattern recognition (leading to random mating behavior), and M_a, M_b and M_c coding for a specific recognition of color pattern phenotypes [A], [B] and [C]. The 'no preference' allele M_r is recessive over all the preference alleles M_a, M_b and M_c, and preference alleles are co-dominant, so that that heterozygotes at the locus M can recognize two different alleles. Then, the recognition enabled by preference alleles M_a, M_b and M_c triggers either attraction (hyp.2.a) or repulsion (hyp.2.b) toward the recognized

color pattern, leading to assortative or disassortative mating behavior depending on the genotype at locus M (see figure S2 and S3 for more details).

We expect the evolution of disassortative mating to be favored when preference alleles (M_a, M_b and M_c) generate rejection behavior (hyp.2.b) rather than attraction (hyp.2.a). Disassortative mating of females indeed implies the avoidance of males displaying their color pattern. Such behavior can simply emerge from an haplotype combining allele a at color pattern locus P and M_a at preference locus M assuming the genetic architecture triggering rejection (hyp 2.b). Assuming a genetic architecture generating attraction (hyp 2.a) however, disassortative mating only emerge when females displaying the color pattern phenotype [A] (i.e. with genotypes *aa*, *ab* or *ac*) carry the heterozygous genotype M_bM_c at the preference locus M, preventing a complete fixation of this behavior.

To characterize female mating preferences generated by the different genotypes at locus M and the link with their own colour pattern phenotype, we distinguish two main behaviors emerging under hyp.2 (fig. S2 and S3 for attraction (hyp.2.a) and rejection (hyp.2.b) hypotheses respectively):

- Self-acceptance : females mate with males displaying their own color pattern phenotype.
- Self-avoidance : females do not mate with males displaying their own color pattren phenotype.

These two inferred behaviours can be directly compared with empirically-estimated mate preferences expressed by females exhibiting different colour patterns, towards males displaying various colour pattern (Chouteau et al., 2017).

Reproduction

We also assume a balanced sex-ratio, a carrying capacity K and a growth rate r, all equal in both populations. We name $N^t_{tot,pop}$ the total density of individuals in population pop at time t. Sexual reproduction is computed explicitly. Assuming Mendelian segregation and a recombination at

rate ρ between both locus, the change in the number of individuals with genotype i in population pop due to reproduction is then described as follows:

The frequency of genotype i in population pop (defined as $f^t_{i,pop}$) is first computed. The change in frequency $F^t_{i,pop}$ then consider the frequencies of each genotype in the population, mendelian segregation and the mate preferences computed in equation 1.4. We assume a single choosy sex: only females can express preference toward males phenotype while males have no preference, and can mate with any accepting females, so that the genotype of the choosy partners i is entirely determining the probability of crosses between partners i and j.

The preference matrix $Pref$ is initially set as $Pref_{i,[j]} = 1$ when females with genotype i accept males with genotype j as mating partner and $Pref_{i,[j]} = 0$ otherwise.

We define the fertility of the individual i as below

$$f_i = Pref_{i,A}P_A + Pref_{i,B}P_B + Pref_{i,C}P_C \tag{4}$$

Where P_i refer to the proportion of the morph i in the population.

Because choosy individuals might have a reduced reproductive success due to limited mate availability (Kirkpatrick and Nuismer, 2004), we also assume a cost associated with choosiness refer to as $cost$, When this cost is low ($cost = 0$), females have access to a large number of potential mates, so that their fertility is not limited when they become choosy ("Animal" model), whereas when this cost is high ($cost = 1$), females have access to a limited number of potential mates, so that their fertility tends to decrease when they become choosy ("Plant" model). This cost of choosiness is known to limit the evolution of mating preferences (Otto et al., 2008).

$$F^{t+1}_{i,pop} = \sum_{j,k} coef(i,j,k,\rho)\frac{1 - cost + cost f_j}{f_j} Pref_{j[k]} \frac{f^t_{j,pop}}{2}\frac{f^t_{k,pop}}{2} \tag{5}$$

Where $coef$ controls the mendelian segregation of alleles during reproduction between an individual of genotype j and an individual of genotype k, therefore depending on the recombination rate ρ between the color pattern locus P and the preference locus M.

We normalized this matrix as $\forall i \sum_j f_{j,pop}^{t+1} = 1$

$$f_{i,pop}^{t+1} = \frac{F_{i,pop}^{t+1}}{\sum_j F_{j,pop}^{t+1}} \tag{6}$$

Overall, the change in the number of genotype i in population pop is given by:

$$\Delta R_{i,pop}^{t} = r(1 - \frac{N_{tot,pop}^{t}}{K}) N_{i,pop}^{t} f_{i,pop}^{t+1} \tag{7}$$

Survival

We assume a mortality rate of larvae named δ. The recessive genetic loads δ_1, δ_2, δ_3 associated with the alleles a, b and c respectively then limits the survival probabilities of larvae with an homozygous genotype at the supergene P. Dominant alleles are usually derived alleles associated with inversions (see Llaurens et al. (2017) for a review) whereas recessive alleles are generally carried by the ancestral gene order. We thus expect that the genetic load associated with the most dominant allele a and the intermediately dominant allele b have similar strength because of deleterious mutations captured by the inversions, i.e. $\delta_1 = \delta_2$. These genetic loads associated with dominant alleles could then be higher than the genetic load associated with the recessive allele c, namely δ_3.

$$\delta_i = \begin{cases} \delta_1 & \text{if } (m_1, m_2) = (a, a) \\ \delta_2 & \text{if } (m_1, m_2) = (b, b) \\ \delta_3 & \text{if } (m_1, m_2) = (c, c) \\ 0 & \text{else} \end{cases} \tag{8}$$

$$\Delta S_{i,pop}^{t} = -(1 - (1 - \delta)(1 - \delta_i)) N_{i,pop}^{t} \tag{9}$$

Tracking the evolution of the two populations using numerical analyses

Overall, the change in the number of genotype i in the population pop is given by:

Abbreviation	Name	Parameter range
N_i^0	Initial size of the population i	100
d	Predation strength	[0,1]
σ	Spatial heterogeneity of local mimicry ring	0.5
λ	Unpalatability coefficient	0.0002
mig	Migration rate	[0,1]
ρ	Recombination rate	[0, 0.5]
r	Growth rate	2
K	Carrying capacity	2000
δ	Baseline death rate	[0, 1]
δ_i	Genetic load linked to allele i	[0, 1]
$cost$	cost of choosiness	[0, 1]
Δf^t	Temporal variations	

Table 1: **Description of parameters used in the model and range explored in simulations.**

$$\Delta N_{i,pop}^t = \Delta P_{i,pop}^t + \Delta R_{i,pop}^t + \Delta M_{i,pop}^t + \Delta S_{i,pop}^t \tag{10}$$

All parameters and range values used in the different simulations are summarized in Table 1 below. Simulations were performed using Python v.3.

The complexity of this two-locus diploid model prevents comprehensive exploration with analytical methods. The model is thus studied using deterministic simulations, to provide general predictions, neglecting the effect of stochastic processes, such as drift. Our predictions might thus be relevant for species with large effective population size, such as *H. numata*. We use discrete time simulations where all events (reproduction, predation and migration) occur simultaneously, therefore relevantly stimulating a natural population with overlapping generations.

In our simulations, the growth rate r is set to 2, the carrying capacity K is assumed to be equal to 2000 per population. Initial population sizes $N^0_{tot,1}$ and $N^0_{tot,2}$ are 100 individuals. The three alleles at the locus P controlling color pattern variations are introduced in proportion $\frac{1}{3}$ in each population. We set the toxicity parameter λ to 0.0002, and the spatial heterogeneity of mimetic communities σ to 0.5. These parameter values are selected as conditions where wing color pattern polymorphism could be maintained without any genetic load or disassortative mating behavior, based on a previous study (Llaurens et al., 2013).

Results

Effect of mate choice on polymorphism

As already highlighted in the literature (Llaurens et al., 2013), assuming random mating, polymorphism can be maintained through an equilibrium between spatially heterogeneous selection and migration. In the absence of migration, alleles *a* and *b* become fixed in population 1 and 2 respectively, owing to their mimetic advantage within their respective communities. Polymorphism with persistence of alleles *a* and *b* within each patch can only be maintained with migration at an intermediate rate, but in all cases the non mimetic allele *c* is lost in both populations (fig.1 (a)).

To test for an effect of mate choice on the previously described selection/migration equilibrium, simulations were carried out introducing alleles (*r*, *dis* or *sim*) at the mate choice locus (Hyp.1), assumed to be fully linked to the colour pattern locus (ρ= 0). We then computed the evolution of frequencies at the color pattern locus after 10,000 time steps for different migration rates *mig*. Assuming assortative mating via self-referencing (hyp. 1) leads to the fixation of the dominant allele *a* in both patches for all migration rates explored, because allele *a* is the most frequently expressed due to dominance and therefore benefits from a frequency-dependent advantage (fig.1 (b)). By contrast, disassortative mating maintains higher degree of polymorphism, with the two mimetic alleles *a* and *b*, and the non-mimetic allele *c* persisting within populations, for all migration rates. The non-mimetic phenotype [C] is rarely expressed because the recessive

allele *c* persists at low frequency, yet associates with high reproductive success because of disassortative mating. Indeed, the strict disassortative preference assumed here strongly increases the reproductive success of individuals displaying a rare phenotype, such as [C]. This effect would be weakened with less stringent mate preferences. Nevertheless, the negative FDS on color pattern generated by disassortative mating counteracts the positive FDS due to predator behavior acting on the same trait. Disassortative mate preferences can thus promote the polymorphism of alleles within and between patches.

Linked genetic load favors the persistence of a non-mimetic allele

In the following simulations, migration parameter *mig* were then set to 0.1, allowing a persistence of polymorphism of alleles *a* and *b* at the color pattern locus *P*, when assuming random mating. We then investigated the influence of a genetic load associated with the different color pattern alleles on polymorphism at the color pattern locus. This allows inferring the effect on polymorphism of heterozygote advantage generated by genetic load, independently of the evolution of mating preferences. We observe that phenotypes [A] and [B] are maintained but not phenotype [C] when a genetic load is associated with the non mimetic allele *c* only ($\delta_1 = \delta_2 = 0$ and $\delta_3 > 0$) or when this load is stronger than the one associated with alleles *a* and *b* (Supp. table S4). However, the non-mimetic allele *c* is maintained with the other alleles *a* and *b* within both populations, when (i) all three alleles carry a genetic load of similar strength, *i.e.* $\delta_1 = \delta_2 = \delta_3 > 0$ or (ii) when allele c is the only one not carrying a genetic load ($\delta_1 = \delta_2 > 0$ and $\delta_3 = 0$) (Supp. table S4). Heterozygote advantage generated by the genetic load associated with mimetic alleles at the locus *P* thus favors the persistence of balanced polymorphism and more specifically promotes the maintenance of the non mimetic allele *c* within both populations.

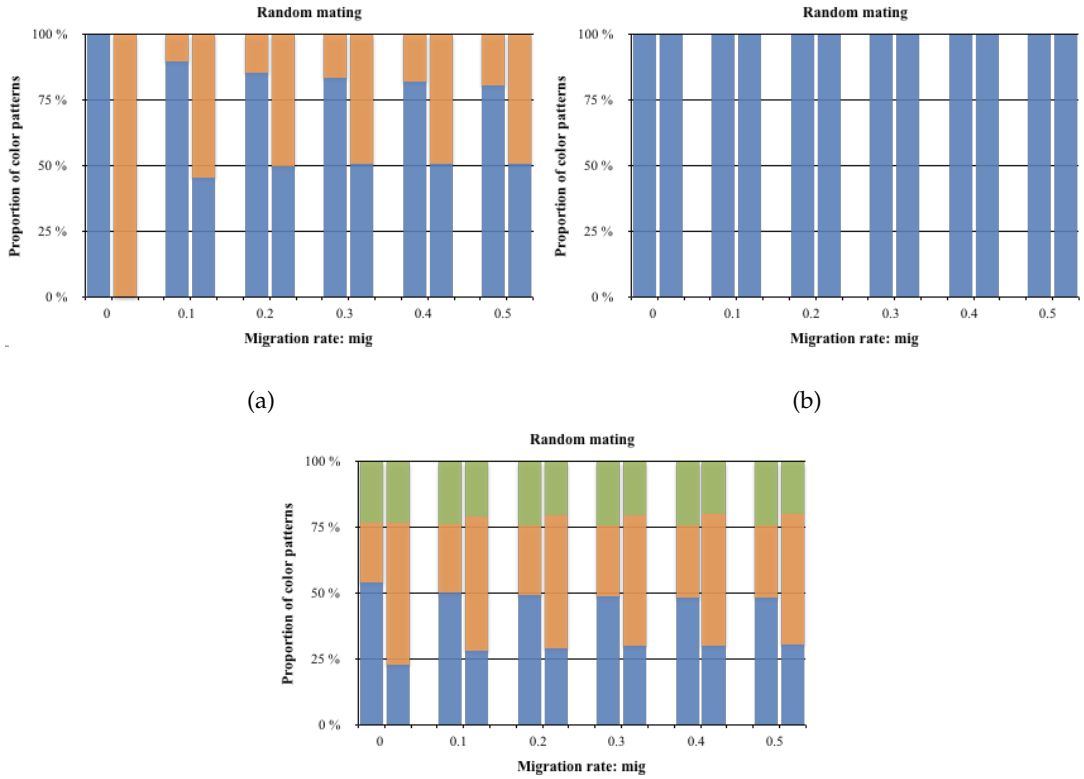

Figure 1: **Impact of mate preferences on color pattern diversity within both populations**. The equilibrium frequencies of color pattern phenotypes in population 1 and 2 for different migration rates *mig* are computed assuming different mating behaviors, *i.e.* assortative (a), random (b) or disassortative (c). The heights of the colored stacked bars indicates the frequencies of color pattern phenotypes [A], [B] and [C] (as blue, orange and green areas respectively) in population 1 and 2 (on the left and right side respectively, within each level of migration). The three alleles at the locus P controlling color pattern variations are introduced in proportion $\frac{1}{3}$ in each population. The locus M controls for the self-referencing based mate preferences (hyp. 1). Simulations are run assuming $r = 2$, $K = 2000$, $N^0_{tot,1} = N^0_{tot,2} = 100$, $\lambda = 0.0002$, $\sigma = 0.5$, $d = 0$, $\rho = 0$, $cost = 0.1$, $\delta_1 = \delta_2 = \delta_3 = 0$ and $\delta = 0$.

Evolution of disassortative mating

Because we expect heterozygote advantage at color pattern locus P to enhance the evolution of disassortative mating preferences at the locus M, we first investigated the influence of a genetic load on the evolution of disassortative behavior, by testing the invasion of mutant inducing self-avoidance (hyp. 1) in a population initially performing random mating. We computed the

frequency of the mutants 100 time steps after the introduction, assuming full linkage between loci P and M. Figure 2 shows that the genetic load associated with alleles a and b ($\delta_1 = \delta_2$) has a strong positive impact on the emergence of disassortative mating. The genetic load associated with the recessive allele c (δ_3) has a slighter positive effect on the evolution of disassortative mating. At a larger evolutionary scale, this leads to the fixation of the disassortative mating allele dis (see equilibrium after 10,000 time steps in supp. figure S5) when the genetic load associated with the dominant alleles a and b is positive. Simulations assuming different costs associated with choosiness (*cost*) show a similar effect of associated genetic loads, although increasing this cost slows down the invasion of the choosy disassortative mating mutant *dis* (see Sup. fig. S6). Overall, this confirms that genetic load linked to the color pattern locus P favors the evolution of disassortative mating behavior in both populations and further promotes polymorphism at the locus P.

How does the genetic architecture of mating preference influence the evolution of disassortative mating behavior ?

To study the evolution of mating behavior assuming different genetic architecture of mate preferences, we investigated the invasion of mate preference alleles M_r, M_a, M_b and M_c controlling random mating, recognition of phenotype A, B and C respectively (Hyp. 2). We ran simulations for 10,000 time steps in order to compute the equilibrium distribution of haplotypes. We first assumed that loci P and M are fully linked ($\rho = 0$). We compared simulations where mate preference alleles triggered either attraction (Hyp. 2a) or rejection (Hyp. 2b) of the recognized color pattern phenotype (fig.3(a) and fig.3(b) respectively).

When preference alleles cause female attraction to males with a given phenotype (Hyp.2a), we observed high frequencies of haplotypes $a - M_b$ and $b - M_a$ in both populations at equilibrium, as soon as the genetic load associated with dominant alleles δ_1 and δ_2 was greater than from 0 (fig.3(a)). These two haplotypes benefit from both positive selection associated with mimicry

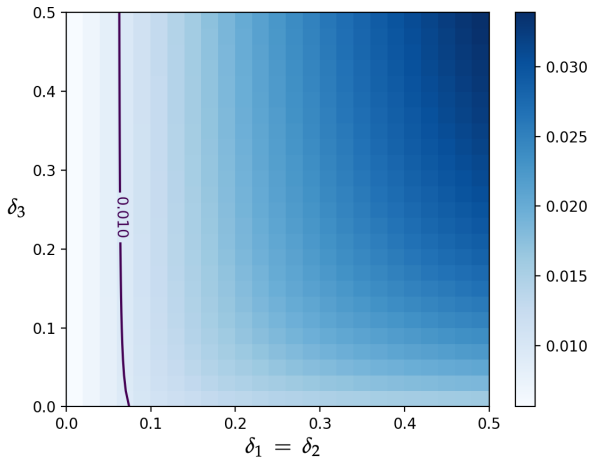

Figure 2: **Impact of linked genetic load on the evolution of disassortative mating, assuming *self-referencing* (Hyp.1).** The invasion of a mutant with disassortative mating preferences depends on the strength of the genetic load associated with dominant alleles a and b assumed equal ($\delta_1 = \delta_2$) (x axis) and with the recessive allele c (δ_3) (y axis). The shade of blue indicates the frequency of the mutant with disassortative mating preferences dis, inducing self-avoidance based on phenotype (hyp. 1), after 100 time steps. The purple line indicates the initial frequency of the mutant, set to 0.01, therefore highlighting the conditios above which an invasion by the mutant is observed. The three alleles at the locus controlling colour pattern variations are introduced in even proportion (*i.e.* $\frac{1}{3}$) in each population, and the initial frequency of the mutant are 0.01, shown by the vertical purple line marking the limit of invasion by the mutant. Simulations are run assuming $r = 2$, $K = 2000$, $N^0_{tot,1} = N^0_{tot,2} = 100$, $\lambda = 0.0002$, $\sigma = 0.5$, $d = 0.1$, $\rho = 0$, $mig = 0.1$, $\delta = 0.1$ and $cost = 0.1$.

and limited expression of the genetic load due to the preferential formation of heterozygotes. Haplotype $c - M_a$ is maintained because of the benefit associated with the choice of the most frequent mimetic phenotype A, and the limited expression of the non-mimetic phenotype C because allele c is recessive. Nevertheless, Haplotype $b - M_a$ becomes lost as the genetic load increases and cannot be compensated by the beneficial effect of mimicry, which is weaker for phenotype B than phenotype A because A is more abundant. As a consequence, the mimetic phenotype B is not maintained in populations where the genetic load is high, and the dominant phenotype A becomes predominantly expressed in both populations.

By contrast, when mate preference is based on alleles causing rejection behavior (Hyp.2b)

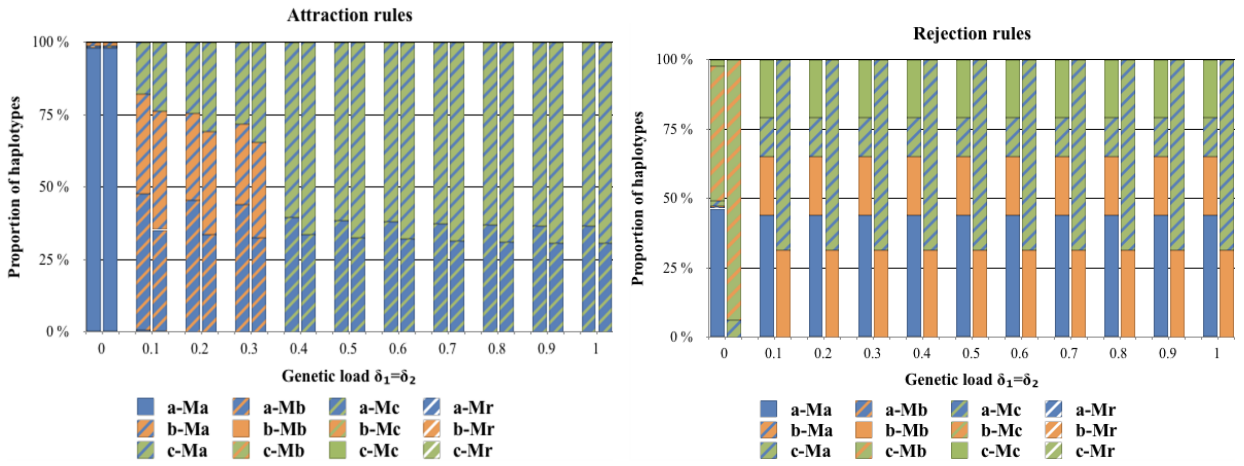

(a) (b)

Figure 3: **Influence of a genetic load on haplotype diversity, assuming (a) attraction rule (hyp. 2a) or (b) rejection rule (hyp. 2b) at the preference locus (*preference/trait*)**. The proportion of haplotypes obtained 2000 time steps after the introduction of preference alleles in both populations are shown for different values of genetic load associated with alleles a and b ($\delta_1 = \delta_2$). The locus M controls for a specific recognition of colour pattern alleles inducing either (a) attraction (hyp.2a) or (b) rejection (hyp.2b). The three alleles at the locus P controlling color pattern variations are initially introduced in even proportion $\frac{1}{3}$ in each population. After 10,000 time steps under random mating the four alleles at locus M: M_r, M_a, M_b and M_c are introduced respectively in proportion 0,99, $\frac{0.01}{3}$, $\frac{0.01}{3}$, $\frac{0.01}{3}$. Simulations are run assuming $r = 2$, $K = 2000$, $N^0_{tot,1} = N^0_{tot,2} = 100$, $\lambda = 0.0002$, $\sigma = 0.5$, $d = 0.1$, $\rho = 0$, $mig = 0.1$, $\delta_3 = 0$, $\delta = 0.1$ and $cost = 0.1$.

and when a genetic load is associated with the mimetic alleles a and b at locus P, these alleles become associated with the corresponding rejection alleles at locus M (*i.e.* $a - M_a$ and $b - M_b$ have an intermediate frequency in both populations) (fig.3(b)). Non mimetic allele c becomes either associated with a self-avoiding allele $c - M_c$, or an allele rejecting the dominant allele a ($c - M_a$). The three alleles (a, b and c) persist within patches for all positive values of genetic load (fig.3(b)). This contrasts with the previously described case where preference alleles lead to attraction (hyp. 2a), for which mimetic allele b is lost when the genetic load is high (fig. 3(a)). Although equilibrium haplotype frequencies are similar for all positive values of genetic load assuming preference allele coding for rejection (Hyp.2b), the strength of genetic load still impacts the temporal dynamics of haplotypes, the equilibrium being reached earlier as the genetic load

increases (see sup. fig S7). This difference in the timing of invasion of the rejection haplotypes reflects higher selection coefficient associated with these haplotypes in simulations where genetic load is stronger.

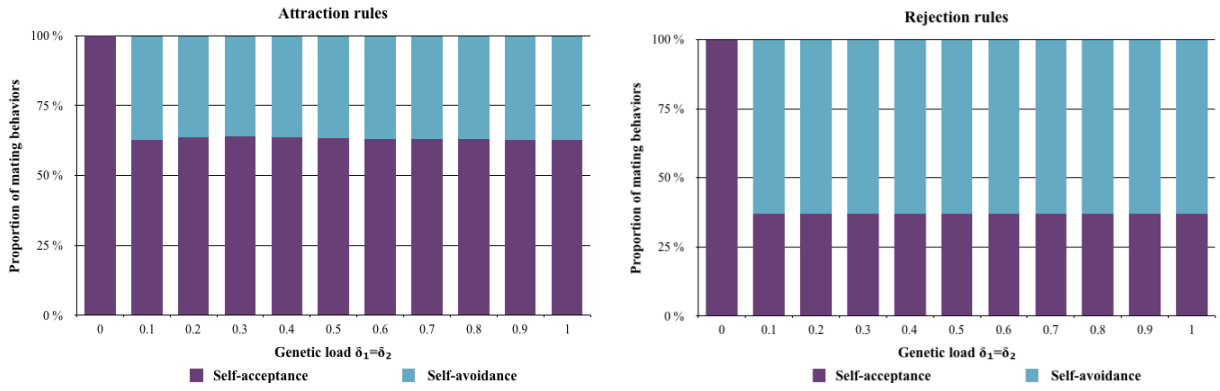

(a) (b)

Figure 4: **Influence of a genetic load on the distribution of mating behaviour observed at the population level, assuming attraction (a) or rejection (b) alleles at the preference locus (*preference/trait*)**. The proportion of individuals displaying self-acceptance (in purple) and self-avoidance (in blue) obtained 2000 time steps after the introduction of preference alleles in both populations are shown for different values of the level of genetic load of δ_1 and δ_2. The locus M controls for a specific recognition of colour pattern alleles inducing either (a) attraction (hyp.2a) or (b) rejection (hyp.2b). The three alleles at the locus P controlling color pattern variations are initially introduced in even proportion $\frac{1}{3}$ in each population. After 10,000 time steps under random mating the four alleles at locus M M_r, M_a, M_b and M_c are introduced respectively in proportion 0,99, $\frac{0.01}{3}$, $\frac{0.01}{3}$, $\frac{0.01}{3}$. Simulations are run assuming $r = 2$, $K = 2000$, $N^0_{tot,1} = N^0_{tot,2} = 100$, $\lambda = 0.0002$, $\sigma = 0.5$, $d = 0.1$, $\rho = 0$, $mig = 0.1$, $\delta_3 = 0$, $\delta = 0.1$ and $cost = 0.1$.

We then investigate how haplotype frequencies translated into individual behavior. When we consider preference alleles leading to attraction (hyp.2a), the majority of individuals display assortative preferences at equilibrium, even with a high genetic load (figure 4(a)). This is surprising given that most haplotypes are of a "disassortative" type, *i.e.* linking a colour pattern allele with an attraction allele to a different colour pattern. Nevertheless, colour pattern alleles b and c are both linked to M_a, coding for attraction to A. As a consequence, most individuals formed are heterozygous at both the colour pattern locus (with one allele a and another allele) and at the preference locus (with one allele coding for attraction to phenotype a and another allele).

These double heterozygotes thus benefit from mimicry but also escape from the expression of deleterious mutations, but can still mate with individuals sharing the same phenotype. By contrast, when we consider preference alleles leading to rejection (hyp.2b), most individuals display a disassortative mating behavior (figure 4(b)). This highlights that the genetic architecture of mate preference plays a key role in the evolution of the mating behavior of diploid individuals and that the evolution of disassortative haplotypes inducing disassortative preferences do not necessarily cause disassortative mating at the population scale.

At equilibrium, the proportion of self-avoidance behavior in the population does not depend of the strength of the genetic load (figure 4(b)). But the strength of the genetic load does impact the speed of evolution of disassortative mating (Supp. fig. S7), and again suggests stronger positive selection on disassortative mating when the genetic load associated with dominant wing colour pattern alleles is higher.

Impact of linkage between loci P and M on the evolution of disassortative mating

We observe that the genetic load associated with the two most dominant alleles at the color pattern locus P impacts the evolution of mate choice, when the color pattern locus P and the preference locus M are fully linked. We then test for an effect of recombination between alleles at the two loci on the evolution of mate choice by performing simulations with different values of the recombination rate ρ. Assuming *self-referencing* (hyp.1), increasing recombination rate further promotes the invasion of the disassortative allele dis (see Sup. fig S8). Under hyp. 1, mate preference depends on the phenotype displayed by the individual, so that the allele *dis* always translates into a disassortative behavior, irrespective of the linkage disequilibrium between preference locus and color pattern locus. Increased recombination thus only results in a more rapid fixation of the disassortative mating allele *dis*, which benefits the associated genetic load. This hypothesis 1 is thus very similar to a single locus architecture, where a single pleiotropic gene controls both the mating cue and the rejection of this cue.

By contrast, when assuming preference for a given color pattern allele (hyp.2), mating be-

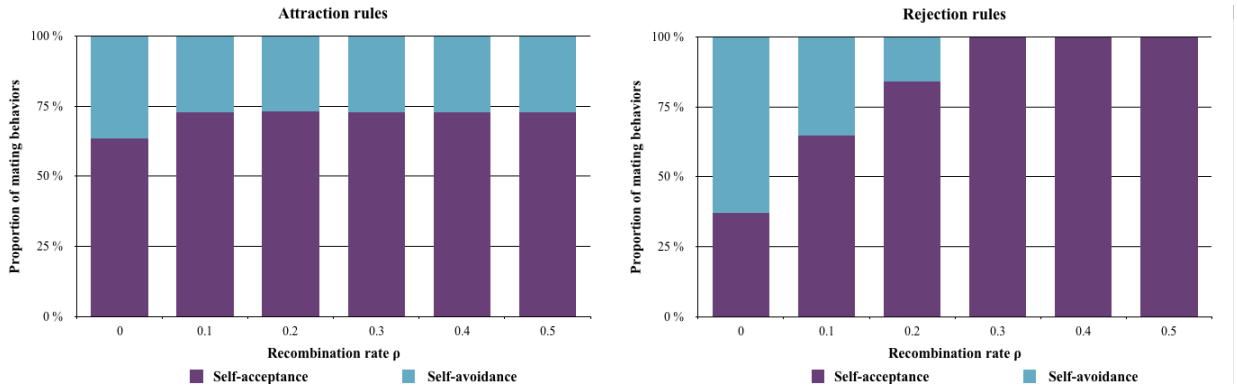

(a) (b)

Figure 5: **Influence of recombination between colour pattern and preference alleles on the distribution of mating behaviours at the population level, assuming (a) attraction or (b) rejection alleles at the preference locus (*preference/trait*)**. The proportion of individuals displaying self-acceptance (in purple) and self-avoidance (in blue) obtained 2000 time steps after the introduction of preference alleles in both populations are shown for different values of recombination rate ρ between the preference locus M and the color pattern locus P. The locus M controls for a specific recognition of colour pattern alleles inducing either (a) attraction (hyp.2a) or (b) rejection (hyp.2b). The three alleles at the locus P controlling color pattern variations are initially introduced in even proportion $\frac{1}{3}$ in each population. After 10,000 time steps under random mating the four alleles at locus M M_r, M_a, M_b and M_c are introduced respectively in proportion 0,99, $\frac{0.01}{3}$, $\frac{0.01}{3}$, $\frac{0.01}{3}$. Simulations are run assuming $r = 2$, $K = 2000$, $N^0_{tot,1} = N^0_{tot,2} = 100$, $\lambda = 0.0002$, $\sigma = 0.5$, $d = 0.1$, $\rho = 0$, $mig = 0.1$, $\delta_3 = 0$, $\delta = 0.1$ and $cost = 0.1$.

havior depends on the genotype at the preference locus M independently of the phenotype of the choosing individuals, so that we expected a stronger effect of recombination rate on mate choice evolution. Figure 5 indeed confirms that, by breaking associations between preference and wing pattern alleles, recombination between locus P and M decreases the proportion of individuals performing self-avoidance at equilibrium. The evolution of disassortative mating behaviors is further impaired when assuming that preference alleles generate rejection (hyp. 2a): self-avoidance behavior completely disappears when preference and colour pattern loci are unlinked (*i.e.* when $\rho = 0.5$).

Under attraction rule (hyp.2.a), for each color pattern allele, two third of the possible haplotypes lead to self-avoidance (for instance $a - M_b$ and $a - M_c$ for color pattern allele a). By

contrast, under rejection rule (hyp.2.b), only one out the three possible haplotypes leads to self-avoidance (for instance $a - M_a$ for color pattern allele a). Moreover, the allele encoding for the rejection of a given color pattern (*e.g.* M_a) is rarely linked with the rejected color pattern allele (*e.g.* a) because mate choice limits crosses between an individual carrying a rejection allele on one hand and an individual displaying the rejected allele on the other hand. This limited linkage between rejecting and rejected alleles further impedes the formation of disassortative haplotypes (*e.g.* $a - M_a$) by recombination when assuming rejection rule (Hyp.2b). Overall, genetic architectures enabling recombination between color pattern and preference loci thus limit the evolution of haplotypes linking colour pattern alleles with the corresponding mate choice allele leading to disassortative mating, when assuming a preference locus acting on the specific recognition of mating cues (*i.e.* under hyp.2).

Discussion

Genetic architecture of disassortative mating: theoretical predictions

Our model shows that disassortative mating is more likely to emerge when genetic architecture is based on *self-referencing* rather than on *preference/trait*. The genetic basis of disassortative mating is largely unknown in natural populations. Assortative mating is better known, for instance in *Heliconius* butterflies where it is generally associated with attraction towards a specific cue. The locus controlling preference for yellow *vs.* white in *H. cydno* maps close to the gene *aristaless*, whose variations in expression controls for the white/yellow switch in this species (Kronforst et al., 2006; Westerman et al., 2018). In *H. melpomene*, a major QTL associated with preference towards red was identified in crosses between individuals displaying a red pattern and individuals with a white pattern (Merrill et al., 2019). This QTL is also located close to the gene optix involved in the variation of red patterning in *H. melpomene*. Assortative mating in *Heliconius* thus seems to rely on alleles encoding for preference for specific cues in linkage with loci involved in the variation of these cues. Contrastingly, our model suggests that the genetic architecture of

disassortative mating might differ from those documented in species showing assortative mating behaviour.

Some *preference/trait* genotypes generate similar mate preferences to some *self-referencing* genotypes: for example, under the rejection rule, the genotype $a - M_a / a - M_a$ leads to the same mate preference as the genotype $a - dis / a - dis$ under self-referencing rule. Introducing recombination in the *preference/trait* rule then enables decoupling the mating cue and its corresponding preference alleles, thereby disrupting the self rejection behaviour. Under the *preference/trait* rule, some haplotypes thus generates partial disassortative mating : for instance the *rejection rule* haplotype $a - Mb$ allows mating with individuals displaying both the non-self phenotype c and the self phenotype a. This self-acceptation behavior may increase the reproductive success associated with these haplotypes. The persistence of these *rejection rule* haplotypes allowing both assortative and disassortative mating prevents the fixation of strict self-rejection behaviour in the population. Furthermore, under the *preference/trait* rule, our model distinguishes whether the specific recognition of the cue leads to either rejection or attraction, and highlights that these two hypotheses lead to evolution of different mate preferences: disassortative mating is indeed more likely to emerge assuming the rejection rule. This rejection rule indeed generates a larger number of self-rejecting haplotypes than the attraction rule, although recombination limits this effect.

Another major difference between the two rules relies on the role of the phenotypes of the choosing and chosen individuals on mate choice. Under both rules, mate choice is based on the phenotype of the chosen individual, so that dominance relationships at the colour pattern locus influences the evolution of disassortative mating. Nevertheless, under *self-referencing*, mate preference also depends on the phenotype of the choosing individual, so that dominance at the colour pattern locus of both the choosing and chosen individuals determines the choice. Under *preference/trait* however, mate preference does not depend on the phenotype of the choosing individual, but on dominance relationships at the mate preference locus, allowing for different types of preference to emerge, including individuals reproducing with different phenotypes only, or individuals mating with either their own phenotype and different ones.

Altogether, our theoretical shows that the genetic basis of mate preferences have a strong impact on the evolution of disassortative mating at loci under heterozygote advantage, pointing out the need to characterize the genetic basis of mate preference empirically, as well as the linkage disequilibrium with the locus controlling variations in the mating cues.

Evolution of disassortative mating results from interactions between dominance and deleterious mutations

Here, we confirm that the evolution of disassortative mating is promoted by the heterozygote advantage associated with alleles determining the mating cue. As mentioned below, the phenotype of the chosen individuals depends on dominance relationships at the colour pattern locus. Our model highlights that a genetic load associated with dominant alleles has as stronger effect on promoting disassortative mating than a genetic load associated with the most recessive haplotype. This theoretical prediction is in accordance with the few documented cases of polymorphism promoted by disassortative mating. In the polymorphic butterfly *Heliconius numata* for instance, the top dominant haplotype *bicoloratus* is associated with a strong genetic load (Jay et al., 2019). Similarly, in the white throated sparrow, the dominant *white* allele is also associated with a significant genetic load (Tuttle et al., 2016). Again, in the self-incompatibility locus of the *Brassicaceae*, dominant haplotypes carry a higher genetic load than recessive haplotypes (Llaurens et al., 2009). Disassortative mating is beneficial because it increases the number of heterozygous offspring with higher fitness. Once disassortative mating is established within populations, recessive deleterious mutations associated with the dominant haplotype become sheltered because the formation of dominant homozygotes is strongly reduced, limiting the opportunities for purging via recombination (Llaurens et al., 2009). Similarly, the model of Karlin and Feldman (1968) suggests that disassortative mating slows down the purge of deleterious alleles. Falk and Li (1969) proved that disassortative mate choice promotes polymorphism, and therefore limits the loss of alleles under negative selection. Disassortative mating might thus shelter deleterious mu-

tations linked to dominant alleles, and thus reinforces heterozygote advantage. The sheltering of deleterious mutations is favoured by the interaction between two aspects of the genetic architecture, dominance at the mating cue locus and limited recombination. This is likely to happen in polymorphic traits involving chromosomal rearrangements, where recombination is limited. Many rearranged haplotypes are indeed associated with serious fitness reduction at homozygotes state (Faria et al., 2019), such as in the derived haplotypes of the supergene controlling controlling plumage and mate preferences in the white-throated sparrow (Thomas et al., 2008). The deleterious elements in inverted segment can be due to an initial capture by the inversions (Kirkpatrick, 2010) but could also accumulate through time, resulting in different series of deleterious mutations associated to inverted and non-inverted haplotypes (Berdan et al., 2019).

Here, we assume that mate choice relied purely on a single cue. Nevertheless, mate choice could be based on other cues, controlled by linked locus and enabling discrimination between homozygotes and heterozygotes, thereby further increasing the proportion of heterozygous offsprings with high fitness. We also modelled strict preferences regarding colour patterns, but choosiness might be less stringent in the wild, and may limit the evolution of disassortative mating. Depending on the cues and dominance relationships among haplotypes, different mate choice behaviours may also evolve, which might modulate the evolution of polymorphism within populations. Our model thus stresses the need to document dominance relationships among haplotypes segregating at polymorphic loci, as well as mate choice behaviour and cues, to understand the evolutionary forces involved in the emergence of disassortative mating.

Conclusions

Inspired by a well-documented case of disassortative mating based on cues subject to natural selection, our model shows that balancing selection promoting local polymorphism and heterozygote advantage is likely to favor the evolution of disassortative mating preferences. The genetic basis of this behavior is predicted to involve haplotypes triggering rejection toward spe-

cific cues. Such rejection loci promote disassortative mating when they are in tight linkage with the locus controlling mating cue variations.

Acknowledgments

The authors would like to thank Charline Smadi and Emmanuelle Porcher for feedback on the modeling approach developed here. We also thank Thomas Aubier and Richard Merrill and the whole Heliconius group for stimulating discussion on mate choice evolution in our favorite butterflies. We are also grateful to Roger Butlin for his thoughtful review of a previous version of this manuscript. This work was supported by the Emergence program from Paris City Council to VL and the ANR grant SUPERGENE to MJ.

References

M. Arias, A. Meichanetzoglou, M. Elias, N. Rosser, D. L. De-Silva, B. Nay, and V. Llaurens. Variation in cyanogenic compounds concentration within a heliconius butterfly community: does mimicry explain everything? BMC evolutionary biology, 16(1):272, 2016.

E. L. Berdan, A. Blanckaert, R. K. Butlin, and C. Bank. Muller's ratchet and the long-term fate of chromosomal inversions. bioRxiv, 2019. 10.1101/606012. URL `https://www.biorxiv.org/content/early/2019/04/13/606012`.

R. K. Butlin, P. M. Collins, and T. H. Day. The effect of larval density on an inversion polymorphism in the seaweed fly coelopa frigida. Heredity, 1984.

L. Casselton. Mate recognition in fungi. Heredity, 88(2):142, 2002.

M. Chouteau, M. Arias, and M. Joron. Warning signals are under positive frequency-dependent selection in nature. Proceedings of the national Academy of Sciences, 113(8):2164–2169, 2016.

M. Chouteau, V. Llaurens, F. Piron-Prunier, and M. Joron. Polymorphism at a mimicry supergene

maintained by opposing frequency-dependent selection pressures. Proceedings of the National Academy of Sciences, 114(31):8325–8329, 2017.

T. H. Day and Butlin. Non-random mating in natural populations of the seaweed fly, coelopa frigida. Heredity, 1987.

M. de Cara, N. Barton, and M. Kirkpatrick. A model for the evolution of assortative mating. The American Naturalist, 171(5):580–596, 2008. 10.1086/587062. URL https://doi.org/10.1086/587062. PMID: 18419568.

C. T. Falk and C. C. Li. Negative assortative mating: Exact solution to a simple model. Genetics, 1969.

R. Faria, K. Johannesson, R. K. Butlin, and A. M. Westram. Evolving inversions. Trends in ecology & evolution, 2019.

S. J. Hiscock and S. M. McInnis. Pollen recognition and rejection during the sporophytic self-incompatibility response: Brassica and beyond. Trends in plant science, 8(12):606–613, 2003.

M. Hori. Frequency-dependent natural selection in the handedness of scale-eating cichlid fish. Science, 260(5105):216–219, 1993.

B. M. Horton, Y. Hu, C. L. Martin, B. P. Bunke, B. S. Matthews, I. T. Moore, J. W. Thomas, and D. L. Maney. Behavioral characterization of a white-throated sparrow homozygous for the zal2 m chromosomal rearrangement. Behavior genetics, 43(1):60–70, 2013.

A. M. Houtman and J. B. Falls. Negative assortative mating in the white-throated sparrow, zonotrichia albicollis: the role of mate choice and intra-sexual competition. Animal Behaviour, 48(2):377–383, 1994.

P. Jay, M. Chouteau, A. Whibley, H. Bastide, V. Llaurens, H. Parrinello, and M. Joron. Mutation accumulation in chromosomal inversions maintains wing pat-

tern polymorphism in a butterfly. bioRxiv, 2019. 10.1101/736504. URL https://www.biorxiv.org/content/early/2019/08/15/736504.

Y. Jiang, D. I. Bolnick, and M. Kirkpatrick. Assortative mating in animals. The American Naturalist, 181(6):E125–E138, 2013. 10.1086/670160. URL https://doi.org/10.1086/670160. PMID: 23669548.

M. Joron and Y. Iwasa. The evolution of a müllerian mimic in a spatially distributed community. Journal of Theoretical Biology, 237(1):87–103, 2005.

M. Joron, I. R. Wynne, G. Lamas, and J. Mallet. Variable selection and the coexistence of multiple mimetic forms of the butterfly heliconius numata. Evolutionary Ecology, 13(7-8):721–754, 1999.

S. Karlin and M. W. Feldman. Further analysis of negative assortative mating. Genetics, 1968.

M. Kirkpatrick. How and why chromosome inversions evolve. PLoS biology, 8(9):e1000501, 2010.

M. Kirkpatrick and S. L. Nuismer. Sexual selection can constrain sympatric speciation. Proceedings of the Royal Society of London. Series B: Biological Sciences, 271(1540):687–693, 2004.

M. Kopp, M. R. Servedio, T. C. Mendelson, R. J. Safran, R. L. Rodríguez, M. E. Hauber, E. C. Scordato, L. B. Symes, C. N. Balakrishnan, D. M. Zonana, et al. Mechanisms of assortative mating in speciation with gene flow: connecting theory and empirical research. The American Naturalist, 191(1):1–20, 2018.

M. R. Kronforst, L. G. Young, D. D. Kapan, C. McNeely, R. J. O'Neill, and L. E. Gilbert. Linkage of butterfly mate preference and wing color preference cue at the genomic location of wingless. Proceedings of the National Academy of Sciences, 103(17):6575–6580, 2006.

Y. Le Poul, A. Whibley, M. Chouteau, F. Prunier, V. Llaurens, and M. Joron. Evolution of dominance mechanisms at a butterfly mimicry supergene. Nature Communications, 5:5644, 2014.

V. Llaurens, L. Gonthier, and S. Billiard. The sheltered genetic load linked to the s locus in plants: new insights from theoretical and empirical approaches in sporophytic self-incompatibility. Genetics, 183(3):1105–1118, 2009.

V. Llaurens, S. Billiard, and M. Joron. The effect of dominance on polymorphism in müllerian mimicry. Journal of theoretical biology, 337:101–110, 2013.

V. Llaurens, A. Whibley, and M. Joron. Genetic architecture and balancing selection: the life and death of differentiated variants. Molecular ecology, 26(9):2430–2448, 2017.

C. Mérot, V. Llaurens, E. Normandeau, L. Bernatchez, and M. Wellenreuther. Balancing selection via life-history trade-offs maintains an inversion polymorphism in a seaweed fly. bioRxiv, 2019. 10.1101/648584. URL `https://www.biorxiv.org/content/early/2019/05/24/648584`.

R. M. Merrill, K. K. Dasmahapatra, J. Davey, D. Dell'Aglio, J. Hanly, B. Huber, C. D. Jiggins, M. Joron, K. Kozak, V. Llaurens, et al. The diversification of heliconius butterflies: what have we learned in 150 years? Journal of Evolutionary Biology, 28(8):1417–1438, 2015.

R. M. Merrill, P. Rastas, S. H. Martin, M. C. Melo, S. Barker, J. Davey, W. O. McMillan, and C. D. Jiggins. Genetic dissection of assortative mating behavior. PLoS biology, 17(2):e2005902, 2019.

F. Müller. Ituna and thyridia; a remarkable case of mimicry in butterflies (transl. by ralph meldola from the original german article in kosmos, may 1879, 100). Transactions of the Entomological Society of London, 1879.

S. P. Otto, M. R. Servedio, and S. L. Nuismer. Frequency-dependent selection and the evolution of assortative mating. Genetics, 179(4):2091–2112, 2008.

D. J. Penn and W. K. Potts. The evolution of mating preferences and major histocompatibility complex genes. The American Naturalist, 153(2):145–164, 1999.

S. Piertney and M. Oliver. The evolutionary ecology of the major histocompatibility complex. Heredity, 96(1):7, 2006.

M. Schilthuizen, P. G. Craze, A. S. Cabanban, A. Davison, J. Stone, E. Gittenberger, and B. Scott. Sexual selection maintains whole-body chiral dimorphism in snails. Journal of evolutionary biology, 20(5):1941–1949, 2007.

T. N. Sherratt. Spatial mosaic formation through frequency-dependent selection in müllerian mimicry complexes. Journal of Theoretical Biology, 2006.

T. Takahashi and M. Hori. Evidence of disassortative mating in a tanganyikan cichlid fish and its role in the maintenance of intrapopulation dimorphism. Biology Letters, 4(5):497–499, 2008. 10.1098/rsbl.2008.0244. URL https://royalsocietypublishing.org/doi/abs/10.1098/rsbl.2008.0244.

X. Thibert-Plante and S. Gavrilets. Evolution of mate choice and the so-called magic traits in ecological speciation. Ecology letters, 16, 06 2013. 10.1111/ele.12131.

J. W. Thomas, M. Cáceres, J. J. Lowman, C. B. Morehouse, M. E. Short, E. L. Baldwin, D. L. Maney, and C. L. Martin. The chromosomal polymorphism linked to variation in social behavior in the white-throated sparrow (zonotrichia albicollis) is a complex rearrangement and suppressor of recombination. 179(3):1455–1468, 2008. ISSN 0016-6731. 10.1534/genetics.108.088229. URL https://www.genetics.org/content/179/3/1455.

T. Tregenza and N. Wedell. Genetic compatibility, mate choice and patterns of parentage: invited review. Molecular Ecology, 9(8):1013–1027, 2000.

E. M. Tuttle, A. O. Bergland, M. L. Korody, M. S. Brewer, D. J. Newhouse, P. Minx, M. Stager, A. Betuel, Z. A. Cheviron, W. C. Warren, et al. Divergence and functional degradation of a sex chromosome-like supergene. Current Biology, 26(3):344–350, 2016.

C. Wedekind and S. Füri. Body odour preferences in men and women: do they aim for specific mhc combinations or simply heterozygosity? Proceedings of the Royal Society of London. Series B: Biological Sciences, 264(1387):1471–1479, 1997.

C. Wedekind, T. Seebeck, F. Bettens, and A. J. Paepke. Mhc-dependent mate preferences in humans. Proceedings of the Royal Society of London. Series B: Biological Sciences, 260(1359): 245–249, 1995.

E. L. Westerman, N. W. VanKuren, D. Massardo, A. Tenger-Trolander, W. Zhang, R. I. Hill, M. Perry, E. Bayala, K. Barr, N. Chamberlain, et al. Aristaless controls butterfly wing color variation used in mimicry and mate choice. Current Biology, 28(21):3469–3474, 2018.

S. Wright. The distribution of self-sterility alleles in populations. Genetics, 24(4):538, 1939.

654

Supplementary Material

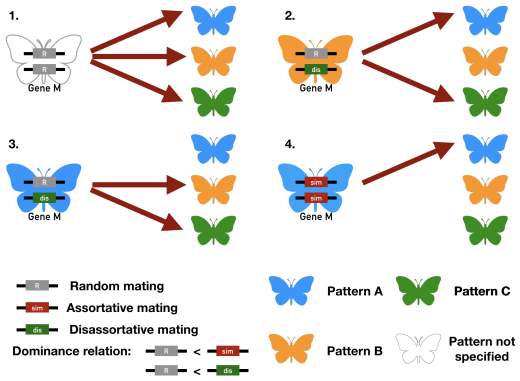

Figure S1: **Mate preferences expressed by the different genotypes at locus *M*, assuming *self-referencing* (Hyp.1).** 1. Butterflies carrying two *r* alleles mate at random, independently from either their own color pattern or the color pattern displayed by mating partners. 2-3. Butterflies carrying a *dis* allele display disassortative mating behavior, and mate preferentially with individuals whose color pattern differ from their own. 4. Butterflies carrying a *sim* allele display an assortative mating behavior and thus preferentially mate with individuals displaying the same color pattern. Cases 1 and 4 therefore lead to *self-acceptance*, while cases 2 and 3 lead to *self-avoidance*.

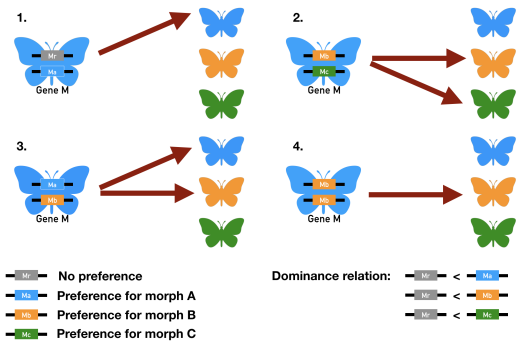

Figure S2: **Mate preferences expressed by the different genotypes at locus *M* assuming preference allele encoding for attraction of specific color patterns (*preference*/*trait*) (hyp.2.a)**. 1. A butterfly displaying phenotype [A] (in blue) carried one allele coding for specific attraction toward partner displaying phenotype [A] (in blue) and the allele coding for random mating at the locus M controlling the mate choice. This butterfly will mate preferentially with individuals displaying phenotype [A], resulting in assortative mating. 2. A butterfly displaying phenotype [A] (in blue) carries one allele coding for specific attraction toward partner displaying phenotype [B] (in orange) and one allele coding for specific attraction toward partner displaying phenotype [C] (in green). This individual will preferentially mate with individuals displaying phenotype [B] and [C], resulting in disassortative mating 3. A butterfly displaying phenotype [A] (in blue) carries one allele coding for specific attraction toward partner displaying phenotype [A] (in blue) and one allele coding for specific attraction toward partner displaying phenotype [B] (in orange). This individual will preferentially mate with individuals displaying phenotype [A] and [B] 4. A butterfly displaying phenotype [A] (in blue) carries two alleles coding for specific attraction toward partner displaying phenotype [B] (in orange). This individual will preferentially mate with individuals displaying phenotype [B], resulting in disassortative mating. Cases 1 and 3 therefore lead to *self-acceptance*, while cases 2 and 4 lead to *self-avoidance*.

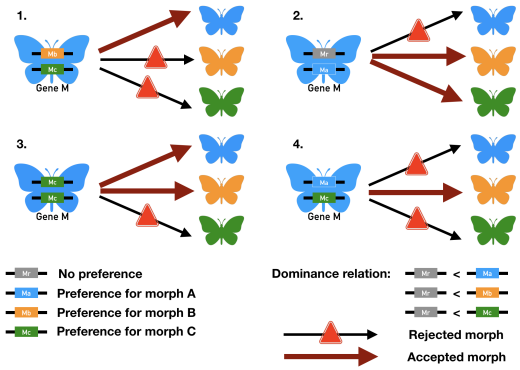

Figure S3: **Mate preferences expressed by the different genotypes at locus *M* preference allele encoding for rejection of specific color patterns (*preference/trait*) (hyp.2.a)**. 1. A butterfly displaying phenotype [A] (in blue) carried one allele coding for specific rejection toward partner displaying phenotype [B] (in orange) and one allele one allele coding for specific rejection toward partner displaying phenotype [C] (in orange). This butterfly will mate preferentially with individuals displaying phenotype [A], resulting in assortative mating. 2. A butterfly displaying phenotype [A] (in blue) carried one allele coding for specific rejection toward partner displaying phenotype [A] (in orange) and one allele coding for random mating (in grey). This butterfly will mate preferentially with individuals displaying phenotypes [B] and [C], resulting in disassortative mating. 3. A butterfly displaying phenotype [A] (in blue) carried two alleles coding for specific rejection toward partners displaying phenotype [C] (in green). This butterfly will mate preferentially with individuals displaying phenotypes [A] and [B]. 4. A butterfly displaying phenotype [A] (in blue) carried one allele coding for specific rejection toward partner displaying phenotype [A] (in blue) and one allele coding for specific rejection toward partner displaying phenotype [C] (in green). This butterfly will mate preferentially with individuals displaying phenotype [B] resulting in disassortative mating. Cases 1 and 3 therefore lead to *self-acceptance*, while cases 2 and 4 lead to *self-avoidance*.

$\delta_1 = \delta_2$	δ_3	Population 1			Population 2		
		Proportion of morph A	Proportion of morph B	Proportion of morph C	Proportion of morph A	Proportion of morph B	Proportion of morph C
0,00	0,00	90 %	10 %	0 %	46 %	54 %	0 %
0,00	0,25	90 %	10 %	0 %	46 %	54 %	0 %
0,00	0,50	90 %	10 %	0 %	46 %	54 %	0 %
0,00	1,00	90 %	10 %	0 %	46 %	54 %	0 %
0,25	0,00	63 %	8 %	28 %	22 %	53 %	25 %
0,25	0,25	79 %	18 %	3 %	35 %	59 %	6 %
0,25	0,50	80 %	18 %	2 %	38 %	58 %	4 %
0,25	1,00	82 %	18 %	1 %	41 %	57 %	2 %
0,50	0,00	56 %	7 %	37 %	19 %	51 %	31 %
0,50	0,25	76 %	19 %	5 %	32 %	59 %	9 %
0,50	0,50	78 %	19 %	3 %	36 %	59 %	5 %
0,50	1,00	80 %	19 %	1 %	39 %	58 %	3 %
1,00	0,00	51 %	5 %	43 %	17 %	48 %	35 %
1,00	0,25	74 %	19 %	7 %	31 %	58 %	11 %
1,00	0,50	77 %	19 %	4 %	35 %	59 %	6 %
1,00	1,00	79 %	19 %	2 %	38 %	58 %	3 %

Figure S4: **Impact of linked genetic load on color pattern polymorphism, assuming random mating.** The proportion of phenotypes [A], [B] and [C] in the population 1 and 2 after 1000 time steps depend on the different values of genetic load associated with the recessive allele c (δ_1), intermediate-dominant allele b (δ_2) and dominant allele c (δ_3). Simulation were run assuming $r = 2$, $K = 2000$, $N^0_{tot,1} = N^0_{tot,2} = 100$, $\lambda = 0.0002$, $\sigma = 0.5$, $d = 0.1$, $\rho = 0$, $mig = 0.1$, $\delta = 0.1$ and $cost = 0.1$.

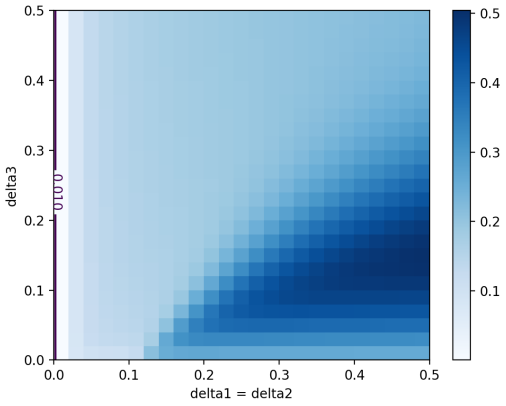

Figure S5: **Effect of the cost of choosiness** *cost* **on the invasion of the disassortative mutant** *dis*, **under the *self-referencing* hypothesis (Hyp.1)**. Simulations are run assuming either low cost of choosiness $cost = 0.1$. The invasion of the disassortative mutant *dis* always depends on the strength of genetic load associated with the dominant alleles a and b ($\delta_1 = \delta_2$) on the x-axis and to the recessive allele c, δ_3, on the y-axis. Level of blue indicates the frequency of the disassortative mutant *dis*, inducing self-avoidance based on phenotype (hyp. 1), after 10,000 time steps.The three alleles at the locus P controlling color pattern variations were introduced in proportion $\frac{1}{3}$ in each population, and the initial frequency of the mutant was 0.01, shown by the vertical purple line, marking the limit of invasion by the mutant. Simulation were run assuming $r = 2$, $K = 2000$, $N^0_{tot,1} = N^0_{tot,2} = 100$, $\lambda = 0.0002$, $\sigma = 0.5$, $d = 0$, $mig = 0.1$ and $\rho = 0$.

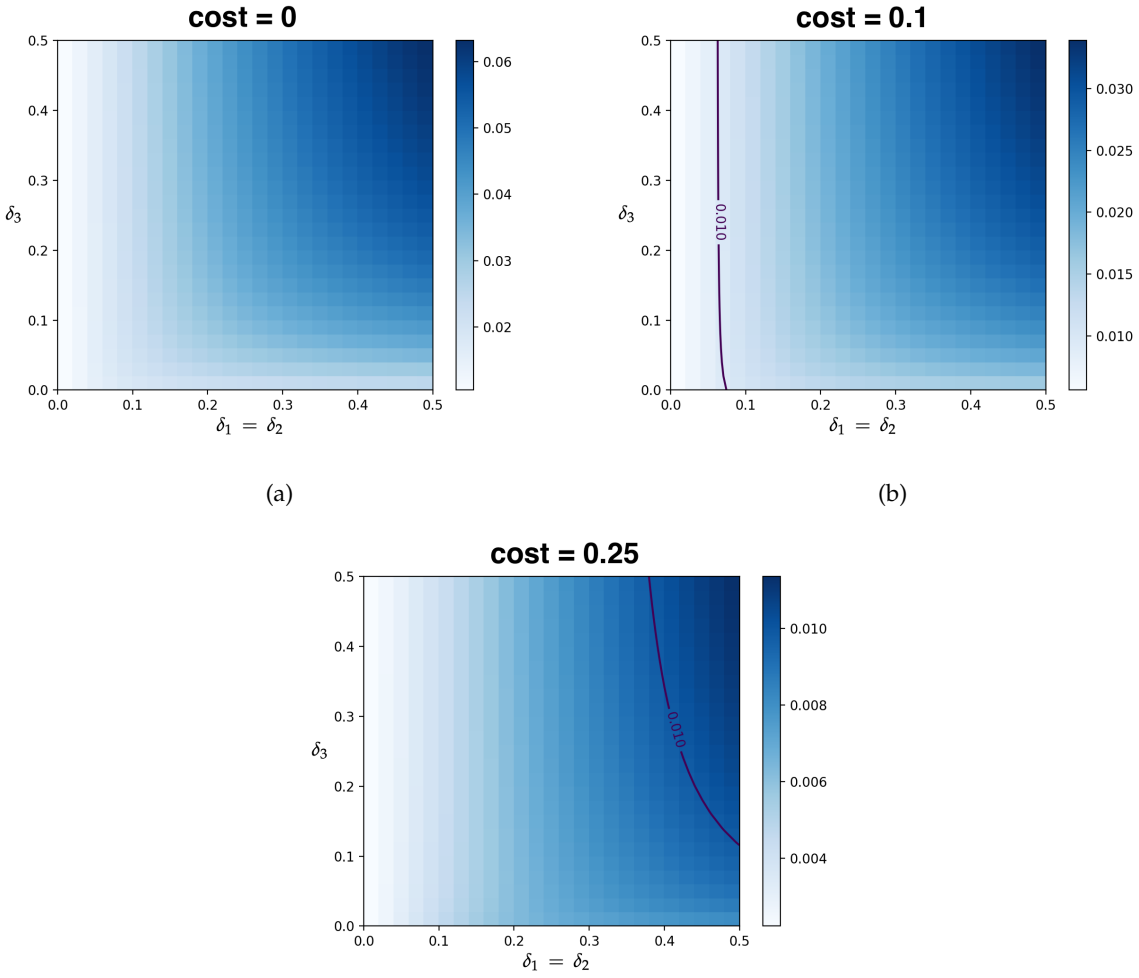

(a) (b)

(c)

Figure S6: **Effect of the cost of choosiness** *cost* **on the invasion of the disassortative mutant** *dis*, **under the** ***self-referencing*** **hypothesis (Hyp.1)**. Simulations were run assuming either *(a)* no cost of choosiness $cost = 0$, *(b)* low cost of choosiness $cost = 0.1$ or *(c)* elevated cost of choosiness $cost = 0.25$. The invasion of the disassortative mutant *dis* always depends on the strength of genetic load associated with the dominant alleles *a* and *b* ($\delta_1 = \delta_2$) on the x-axis and to the recessive allele *c*, δ_3, on the y-axis. Level of blue indicates the frequency of the disassortative mutant *dis*, inducing self-avoidance based on phenotype (hyp. 1), after 100 time steps.The three alleles at the locus *P* controlling color pattern variations were introduced in proportion $\frac{1}{3}$ in each population, and the initial frequency of the mutant was 0.01, shown by the vertical purple line, marking the limit of invasion by the mutant. Simulation were run assuming $r = 2$, $K = 2000$, $N^0_{tot,1} = N^0_{tot,2} = 100$, $\lambda = 0.0002$, $\sigma = 0.5$, $d = 0$, $mig = 0.1$ and $\rho = 0$.

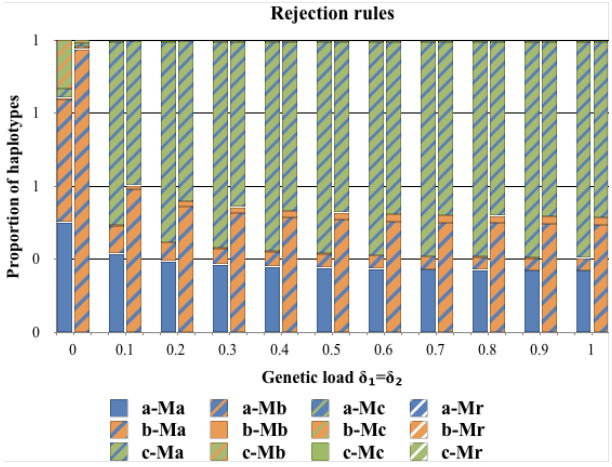

Figure S7: **Impact of the genetic load on haplotype diversity, assuming rejection alleles at the preference locus (Hyp. 2b), during the emergence of preference alleles**. The proportion of haplotypes obtained 200 time steps after the introduction of preference alleles in both populations are shown for different values of genetic load associated with alleles a and b ($\delta_1 = \delta_2$). The locus M controls for a specific recognition of colour pattern alleles inducing either (a) attraction (hyp.2a) or (b) rejection (hyp.2b). The three alleles at the locus P controlling color pattern variations are initially introduced in even proportion $\frac{1}{3}$ in each population. After 10,000 time steps under random mating the four alleles at locus M M_r, M_a, M_b and M_c are introduced respectively in proportion 0,99, $\frac{0.01}{3}$, $\frac{0.01}{3}$, $\frac{0.01}{3}$. Simulations are run assuming $r = 2$, $K = 2000$, $N^0_{tot,1} = N^0_{tot,2} = 100$, $\lambda = 0.0002$, $\sigma = 0.5$, $d = 0.1$, $\rho = 0$, $mig = 0.1$, $\delta_3 = 0$, $\delta = 0.1$ and $cost = 0.1$.

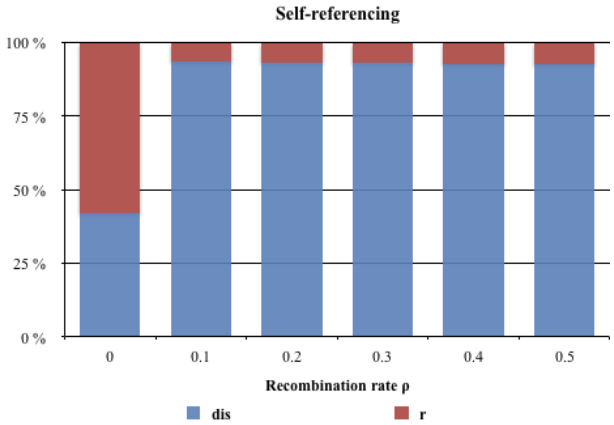

Figure S8: **Impact of recombination between color pattern (locus P) and preference alleles (locus M) on mating behavior, assuming self-referencing preference alleles (Hyp.1).** The proportion of *dis* and *r* alleles in both populations for different values of recombination rate ρ after 10,000 time steps. The three alleles at the locus P controlling color pattern variations were introduced in proportion $\frac{1}{3}$ in each population and the genetic architecture to describe the locus M corresponded to self-referencing (hyp.1). Simulations were run assuming $r = 2$, $K = 2000$, $N^0_{tot,1} = N^0_{tot,2} = 100$, $\lambda = 0.0002$, $\sigma = 0.5$, $d = 0.1$, $mig = 0.1$, $\delta_1 = 0.5$, $\delta_2 = 0.5$ $\delta_3 = 0$, $\delta = 0.1$ and $cost = 0.1$.